Received: 6 January 2016 | Accepted: 8 November 2016

DOI 10.1111/vsu.12628

ORIGINAL ARTICLE

Mechanical properties of canine osteosarcoma-affected antebrachia*

Michele A. Steffey[1] | Tanya C. Garcia[2] | Leticia Daniel[1] | Allison L. Zwingenberger[1] | Susan M. Stover[2]

[1] Department of Surgical and Radiological Sciences, School of Veterinary Medicine, University of California-Davis, Davis, California

[2] Department of Anatomy, Physiology and Cell Biology, School of Veterinary Medicine, University of California-Davis, Davis, California

Correspondence
Michele A. Steffey, Department of Surgical and Radiological Sciences, School of Veterinary Medicine, University of California-Davis, 1 Shields Ave, Davis, CA 95616.
Email: masteffey@ucdavis.edu

Funding information
University of California-Davis Center for Companion Animal Health

Abstract

Objective: To determine the influence of neoplasia on the biomechanical properties of canine antebrachia.

Study design: Ex vivo biomechanical study.

Sample population: Osteosarcoma (OSA)-affected canine antebrachia (n = 12) and unaffected canine antebrachia (n = 9).

Methods: Antebrachia were compressed in axial loading until failure. A load-deformation curve was used to acquire the structural mechanical properties of neoplastic and unaffected specimens. Structural properties and properties normalized by body weight (BW) and radius length were compared using analysis of variance (ANOVA). Modes of failure were compared descriptively.

Results: Neoplastic antebrachia fractured at, or adjacent to, the OSA in the distal radial diaphysis. Unaffected antebrachia failed via mid-diaphyseal radial fractures with a transverse cranial component and an oblique caudal component. Structural mechanical properties were more variable in neoplastic antebrachia than unaffected antebrachia, which was partially attributable to differences in bone geometry related to dog size. When normalized by dog BW and radial length, strength, stiffness, and energy to yield and failure, were lower in neoplastic antebrachia than in unaffected antebrachia.

Conclusions: OSA of the distal radial metaphysis in dogs presented for limb amputation markedly compromises the structural integrity of affected antebrachia. However, biomechanical properties of affected bones was sufficient for weight-bearing, as none of the neoplastic antebrachia fractured before amputation. The behavior of tumor invaded bone under cyclic loading warrants further investigations to evaluate the viability of in situ therapies for bone tumors in dogs.

1 | INTRODUCTION

OSA is the most common primary bone tumor of the dog, with the majority of cases occurring in the appendicular skeleton. Thoracic limbs are more commonly affected than the pelvic limbs; within the forelimb, the metaphysis of the distal radius is most commonly affected.[1] Recommended treatment usually consists of surgical excision of the primary lesion followed by adjuvant chemotherapy. Amputation is the most common surgical procedure recommended for OSA to simultaneously remove neoplastic tissue and alleviate pain, while ensuring low morbidity in terms of dehiscence and infection.[1] However, amputation is not an option for dogs with concurrent disease, where it would create unacceptable functional deficits, or because clients oppose amputation due to personal ethics.

*These data were presented in part at the Veterinary Society of Surgical Oncology Biennial Meeting, February 2015, Napa, CA.

Alternatives to amputation include surgical limb-salvage procedures utilizing autografts, allografts, metal endoprostheses, and bone-transport osteogenesis in dogs with distal radial OSA. These options provide comparable survival times to those after amputation.[1-8] However, complications associated with these procedures are common, including infection (in up to 78% of cases[8]), tumor recurrence (rates as high as 24%[8]), and construct failure (in up to 40% of cases[3]). Limb salvage by curative intent radiation therapy for local tumor control has been described using full-course fractionated therapy, intraoperative extracorporeal radiation therapy, and stereotactic radiosurgery, but resulted in pathologic fractures in up to 60% of cases.[9-13] Dogs undergoing palliative medical care for appendicular OSA have recently been reported to sustain pathologic fractures in 38% of cases, with a median time from diagnosis to euthanasia or death of 111 days.[14] This morbidity justifies efforts to improve our understanding of the biomechanics of tumor-invaded bone as a prerequisite to predict the risk of fractures in veterinary OSA patients.

Management of primary and metastatic appendicular bone neoplasia in humans include a variety of options, ranging from amputation, various forms of surgical limb salvage, or in situ treatment options such as radiation therapy, thermal ablation (eg, cryoablation, microwave ablation, radiofrequency ablation),[15,16] and selective arterial embolization.[17] In situ treatment of neoplasms have been suggested as a strategy to retard metastasis through mechanisms relying on immunologic responses to tumor antigens[18,19] and concomitant tumor resistance.[20,21] Antigenic tissue proteins released from lesions treated in situ under supportive conditions are believed to initiate a systemic immune response directed against the specific tumor, potentially reducing local recurrence and/or pulmonary metastasis.[22,23] Most canine OSA patients ultimately die of metastatic disease distant to their primary tumor.[1] Less-invasive in situ treatments could therefore be more attractive than amputation in these patients, if they can effectively retard tumor spread, while limiting pain and complication rates to acceptable levels.

However, in situ treatment of local bone neoplasia warrants careful extrapolation across species due to differences in 1) skeletal biomechanics, and 2) ease of managing weight bearing modifications in the affected limb. Successful removal of discomfort by radiation, pharmacologic, or other therapies in dogs is likely to result in improved and potentially uncontrolled weight bearing on grossly abnormal bone, thereby increasing the risk of pathologic fracture. In situ therapies for OSA, if confirmed to induce an anti-tumor immune response reducing distant tumor growth, may improve long-term outcomes compared to other limb salvage options, in the subset of canine OSA patients at low risk for pathologic fracture. Early reports have described the successful treatment of pathologic fractures associated with appendicular neoplasia in dogs, as well as pre-emptive support of tumor-bearing bone with internal fixation.[13,24-26] At this time, biomechanical loads leading to pathologic fracture in tumor-bearing bone are unknown in the dog, and no criteria has been established to assess the risk of pathologic fractures in veterinary patients. A better understanding of the biomechanical properties of OSA diseased bones and their ability to withstand weight bearing loads in dogs would provide evidence to support treatment recommendations in candidates for limb salvage.

The purpose of this study is to provide fundamental biomechanical data on tumor-invaded bone in a cohort of dogs with naturally occurring OSA of the distal radius, as a foundation for future work on the likelihood of fracture under physiologic loads. The hypothesis is that the presence of OSA will compromise canine antebrachial stiffness and strength and result in bone fracture at the OSA site.

2 | MATERIALS AND METHODS

2.1 | Study subjects

This study was approved by the Institutional Animal Care and Use Committee, and informed owner consent was obtained prior to study inclusion. A convenience (availability) sample of limbs was collected over a 3-year period. Unpaired forelimbs from 10 client-owned dogs presenting for treatment of unilateral primary OSA of the distal radius with forelimb amputation (and in which there was no evidence of existing pathologic fracture), and unpaired forelimbs from 9 dogs without known orthopedic disorders, euthanatized for reasons other than forelimb musculoskeletal pathology, were studied. Bilateral neoplastic limbs were obtained from 1 additional clinical patient euthanatized due to bilateral OSA lesions in the distal radial metaphyses and poor quality of life. A total of 12 affected antebrachia were therefore obtained from 11 diseased dogs for the study. In the 10 client-owned dogs undergoing amputation, no dog exhibited radiographic or CT evidence of an existing pathologic fracture, all dogs were treated according to clinical standard of care recommendations by the attending clinicians regarding cancer staging, anesthetic drug and monitoring recommendations, and operative/postoperative management, but these aspects of care were not standardized as part of the study protocol. No radiographic evidence of pathologic fracture was detected in the bilaterally affected dog. Diagnosis of OSA was suspected based on aspiration cytology preoperatively, and confirmed in all dogs with histopathology of all tumor-bearing antebrachia.

2.2 | Imaging

Each clinical case underwent CT of both fore limbs under general anesthesia before limb amputation. CT scans of a single limb from each of the 9 cadaveric control antebrachia were performed ex vivo. A CT scan was not obtained in the dog euthanatized for bilateral antebrachial OSA. Axial CT (LightSpeed 16, GE Medical Systems) images were obtained with the long axis of the limbs aligned along the axial dimension of the gantry at 120 kVp and 200 mA at a resolution of 0.625 mm slice thickness and 0.406 mm pixels (512 × 512 pixel matrix). Images were reconstructed using a BONE convolution kernel. A Cann-Genant phantom (CT Calibration Phantom, Mindways Software Inc, San Francisco, California) with 5 known hydroxyapatite densities was placed in the field of view. The head was positioned out of the scan field of view to prevent attenuation artifacts.

2.3 | Specimen preparation and mechanical testing

The 10 limbs obtained from pets with unilateral OSA were tested biomechanically immediately after amputation, and prior to histology. The 9 OSA-free limbs, and both limbs from the dog with bilateral OSA were stored at −20°C in sealed watertight bags until mechanical testing.[27] Axial compressive loading was selected in this study to reproduce physiologic weight-bearing. The radius and ulna were tested as a construct, to simulate a clinical scenario. Indeed, preservation of the ulna increased loads to yield and ultimate failure by 41% and 29%, respectively, in limbs reconstructed with cortical bone grafts, although this difference was not statistically significant.[28] Physiologic loading conditions were estimated from preliminary tests on a strain gauged cadaveric antebrachium from 1 dog. Uni-axial strain gauges were placed on the cranial and caudal sides of the radius, at the mid-diaphysis, with the strain measurement directed along the longitudinal axis of the radius. The test antebrachium was loaded in axial compression with the proximal end of the specimen under 2 conditions: (1) rigidly constrained, followed by (2) un-constrained, thereby allowing rotation in the sagittal plane. In both conditions, rotation of the distal end of the bone was unconstrained to allow bending of the antebrachium. The ratio of cranial-to-caudal strain and magnitude of cranial strain were most consistent with in vivo strain gauge data[29,30] when the proximal end was held rigid (constrained rotation).

The radius and ulna were dissected from the limbs while preserving the interosseous ligament. The proximal ends of the radius and ulna were potted in a 3″ deep metal fixation cup with bone cement (PMMA, Coe Tray Plastic, GC America, Chicago, Illinois) to ensure rigid fixation during mechanical testing. Pins (1/8″ in diameter) were inserted through the radius and ulna cranio-caudally, and through the ulna mediolaterally to stabilize the bones within the PMMA. The longitudinal axis of the bone was aligned with the direction of loading with orthogonal laser beam guides. The proximal ends of the bones were depressed 5 mm deep into a shallow well filled with liquid PMMA. The cement was allowed to set prior to fixing the potted bones rigidly into the mechanical testing system (Model 809, MTS Systems Corp, Minneapolis, Minnesota). The distal fixation prevented translation, but allowed some freedom for rotation (Figure 1). Axial compression was applied at a rate of 1 mm/s until bone failure occurred or when the force decreased to 50% of its maximum. Load and displacement were recorded at 60 Hz. Digital radiographs (lateromedial [LM] and craniocaudal [CrCd] views) were taken before and after tests to characterize the geometry and location of bone failure (48 kVp, 4.6 mAs, Minxray HF 100/30+ generator and Sound-Eklin EDR3 digital control panel).

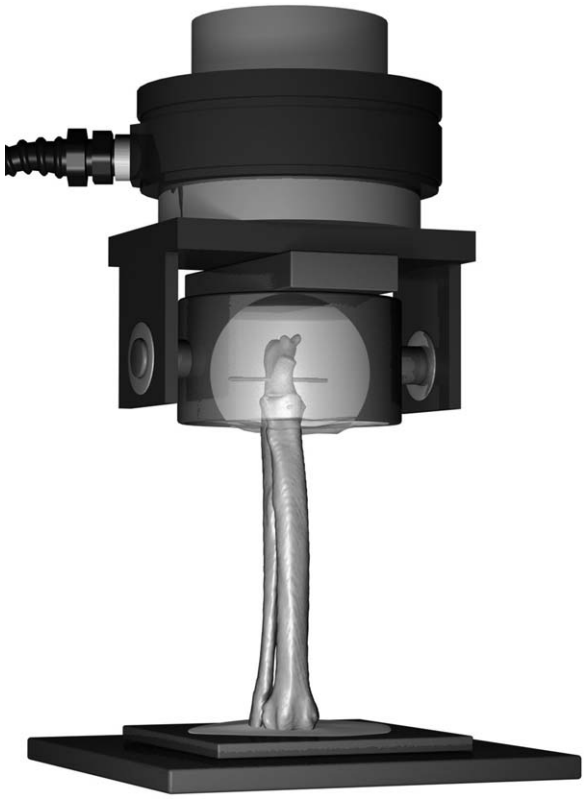

FIGURE 1 Antebrachii are loaded in axial compression by embedding transfixation pins and the proximal end of the antebrachium in polymethylmethacrylate and allowing the distal end of the antebrachium to rotate over an impression of the distal end in polymethylmethacrylate

2.4 | Mechanical testing data reduction

Load-displacement curves were produced from the mechanical testing data. Reduced structural test variables included pre-yield and post-yield stiffness, and load, displacement,

and energy at points of construct yield, maximum load, and failure. Construct yield, where the curve initiates nonlinearity, was determined using a 0.25% displacement offset. The point of maximum strength was the highest load before failure. Failure was defined as the point at which the load decreased rapidly after the point of maximum strength. Pre-yield stiffness was calculated as the slope of the least squares regression for the central third of the data in the linear portion of the curve. Post-yield stiffness was calculated by the slope of the line fit of the central third of the data between yield and maximum strength. The energies to yield, maximum strength, and failure were calculated as the areas under the curve from the beginning of loading to the respective points on the curve. The displacement and energy at a trot load (110% of body weight [BW] in mixed-breed dogs)[31-33] were calculated to capture physiologically relevant values. The type of failure was categorized as oblique, comminuted, transverse, or crushing fractures.

Bone size correlates with the expected magnitude of the structural mechanical properties. To mitigate the effects of dog size on bone properties, data derived from load displacement curves were normalized for dog BW or antebrachial bone length, as described below.

Dogs' BWs were unknown for 4 of 21 specimens and were extrapolated using the best correlation of known BWs with 3 estimates of antebrachial bone size, which were available in all dogs. First, mid-diaphyseal antebrachial bone cross-sectional area (CSA_{ct}) was measured using CT data from a single mid-diaphyseal slice. Second, an estimate of antebrachial bone volume by radiographic measurement (V_e) was estimated by approximating bone CSA at the mid-diaphysis as an ellipse whose width and depth were measured on LM and CrCd radiographs. Antebrachial bone length was measured from the center of the curvature of the trochlear notch of the ulna to the distal extent of the radius.

$$V_e = \frac{\text{width}}{2} \times \frac{\text{depth}}{2} \times \pi \times \text{length}$$

Third, a second estimate of antebrachial bone volume (V_{csa}) by CT measurement was calculated using CSA_{ct} and antebrachial bone length as below.

$$V_{csa} = CSA_{ct} \times \text{length}$$

The best surrogate of BW was determined by assessing the strength of correlations between CSA_{ct}, V_e, and V_{csa} with BW for dogs of known BW. The regression equation for the best correlation was used to estimate BWs for the 4 dogs with unknown BWs. Loads and displacements were normalized for BW and antebrachial bone length, respectively, thereby standardizing variables derived from load displacement curves.

2.5 | Statistical analysis

The strengths of the relationships between CSA_{ct}, V_e, and V_{csa} with BW were assessed using the Pearson correlation statistic. BWs were compared between OSA affected limbs and unaffected limbs using a Wilcoxon test.

Structural mechanical properties were compared between OSA affected and unaffected limbs with a mixed model ANOVA that accounted for the repeated measures in the dog with bilateral OSA. For the non-normalized variables, BW was also included as a covariate. Normality of the residuals from the ANOVA was assessed using a Shapiro Wilks test. For the variables with non-normally distributed residuals, a nonparametric Wilcoxon test was used to assess differences between OSA affected and unaffected limbs. Averages for the left and right limbs of the dog with bilateral OSA were used for the Wilcoxon test. Least square means (LSmeans), standard errors (StdErr), and coefficients of variation (COV) are reported for variables with normally distributed ANOVA residuals. Median, minimum, and maximum values and COV are reported for variables examined using the nonparametric Wilcoxon test. Variables with P values less than .05 were considered statistically significant. Statistical analyses were performed using SAS 9.3 software (SAS Institute, Cary, North Carolina).

3 | RESULTS

3.1 | Clinical data

12 neoplastic limbs (5 left, 7 right) from 11 dogs diagnosed with OSA were tested. Dogs were 7.5 ± 2.5 years (mean ± SD) of age, including 4 female and 8 male dogs, with a median weight of 43 kg, ranging from 32 to 94 kg. Breeds included 2 Mastiffs, 3 Labrador Retrievers, 2 Golden Retrievers, 3 German Shepherds, and 1 Rottweiler mix. Age, breed, and sex were unknown for the cadavers from which the OSA-unaffected limbs (3 left, 6 right) were obtained, but all were large breed dogs. All forelimbs were skeletally mature with no evidence of open growth plates. BWs were measured in 5 cadavers, with a median of 26 kg (range: 21-34 kg). The BW of the remaining 4 donors of cadaver limbs was estimated to range from 21 to 30 kg. Dogs with OSA of the antebrachia weighed more than dogs with unaffected antebrachia (Wilcoxon $P < .001$).

3.2 | Body-weight surrogate

Bone mid-diaphyseal CSA_{ct} had the highest correlation with known dog BWs (n = 16 dogs, R = 0.89, $P < .001$). V_e, and V_{csa} had lower correlations (R = 0.76 and R = 0.84, respectively). The regression equation used to estimate BW was $BW = (CSA_{ct} - 48.4)/6.53$.

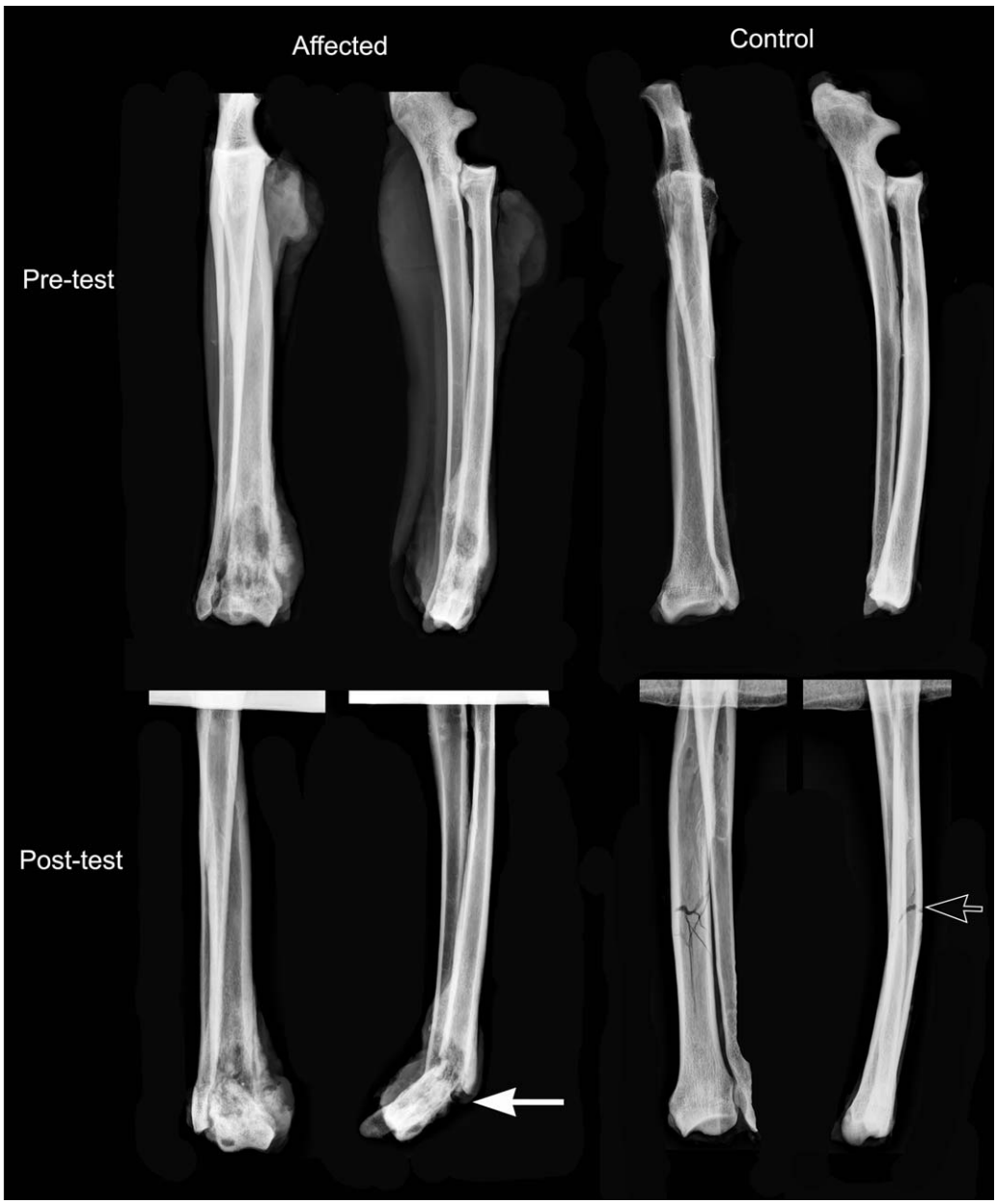

FIGURE 2 Representative craniocaudal (CrCd) and lateromedial (LM) radiographs before (Pre-test) and after (Post-test) axial compression to failure tests for neoplastic and normal control antebrachii. Neoplastic radii exhibited a combination of transverse and crushing type fracture at (n = 11), or just proximal to (n = 1), the OSA (white arrow), whereas all control radii had mid-diaphyseal fractures with transverse components on the cranial side and oblique components on the caudal side, with occasional comminution (open arrow)

3.3 | Failure mode

Eleven out of 12 neoplastic antebrachia failed through a combination of transverse and crushing fractures of the radius within the tumor site, with cranial rotation of the proximal end of the distal fragment (Figure 2). One neoplastic bone had an oblique (proximo-lateral to disto-cranial) radial fracture in the proximal-most portion of the OSA. The other neoplastic bone was collected from the youngest dog (4-year-old) in the study and failed with a comminuted fracture just proximal to the OSA. Each ulna fractured at the same level as the matched neoplastic radius.

All 9 control antebrachia failed by proximocranial to distocaudal radial fractures, with comminution in 2 cases. All fractures were transverse in the cranial cortex, and oblique in the caudal cortex, consistent with bending (Figure 2). The fractures occurred approximately 1/3 to 1/2 of the bone length from the distal end. Ulnar fractures occurred in only 6 control antebrachia, all located at the level as the radial fracture.

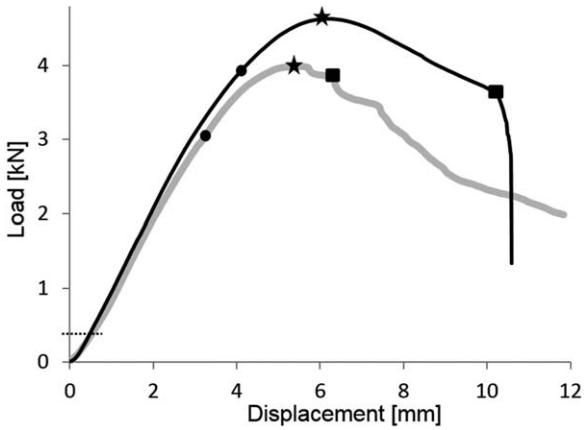

FIGURE 3 Representative load-deformation curves from an neoplastic antebrachium (thick grey line) and an unaffected control antebrachium (thin black line) from dogs of comparable body-weights. Yield, maximum load, and failure points are designated with filled circles, stars, and filled rectangles, respectively. Horizontal dotted line shows approximate load on the limb at a trot

3.4 | Mechanical properties

All specimens exhibited considerable displacement (plasticity) between maximum load and failure (Figures 3 and 4). Whereas load displacement curves were consistent with a smooth plastic behavior in 7 of 9 control bones, the presence of steps after maximum load in neoplastic bones was consistent with decremental failure. Two diseased bones exhibited smooth and fairly stiff behavior after reaching maximum load. One of these bones fractured proximal to the OSA, at a site apparently not affected by neoplasia. The second specimen was the only affected bone that sustained an oblique fracture.

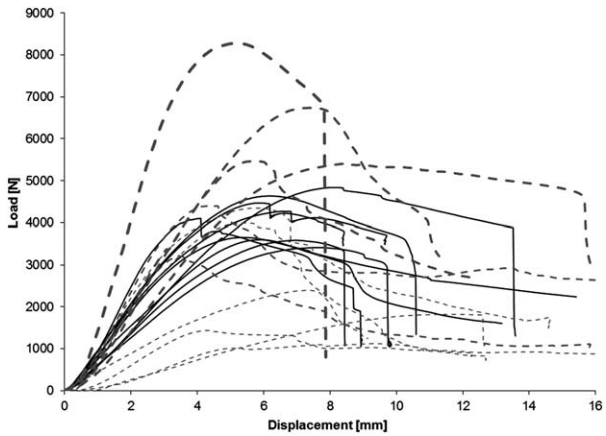

FIGURE 4 Load-deformation curves of all bones tested. Affected limbs are represented by dashed lines, unaffected control limbs are represented by solid lines. Dashed and solid line thickness are proportional to dog weight grouped by weight ranges <30 kg, 31-50 kg, 51-70 kg, >70 kg

The only differences between absolute structural properties were detected at yield: the displacement and mean energy were 28% and 50% lower, respectively, in neoplastic antebrachia than in unaffected antebrachia (Table 1). In addition, all mechanical parameters were more variable in neoplastic antebrachia (coefficient of variation [COV]) than in unaffected bones (Table 1, Figure 4). All neoplastic antebrachia that sustained yield, maximum, and failure loads higher than those of unaffected bones were from heavier dogs (Figure 5). Accordingly, all normalized variables, except trot displacement and energy, differed markedly between neoplastic and control antebrachia (Table 2). Normalized mean or median yield, maximum, and failure loads of neoplastic antebrachia approximated 52%, 54%, and 61%, respectively, of corresponding parameters in unaffected antebrachia. Normalized mean or median trot and yield stiffnesses of neoplastic antebrachia were equal to 34% and 47%, respectively, of those of unaffected bones. Normalized mean or median yield, maximum, and failure displacements of neoplastic antebrachia approximated 67%, 75%, and 59%, respectively, of corresponding values in unaffected specimen. Normalized mean or median yield, maximum, and failure energies of neoplastic antebrachia were 33%, 37%, and 27%, respectively, of those of control antebrachia.

4 | DISCUSSION

The biomechanical testing of tumor bearing antebrachia in dogs with naturally occurring OSA allowed the detection of altered structural properties in these bones, in spite of their great variability in biomechanical properties. Neoplastic antebrachia were markedly weaker, more compliant, and absorbed less energy to yield and failure, than normal antebrachia. These bones also exhibited step-by-step reductions in load after maximum load, consistent with sequential or decremental failures. All neoplastic antebrachia, with one exception, failed by crushing and/or bending at the OSA site, in the distal metaphysis of the radius. This failure pattern indicates that the OSA lesion forms the weakest part of the antebrachium, matching clinical observations described by others.[26] By contrast, normal antebrachia failed by mid-diaphyseal fractures, consistent with bending during axial compression.

The yield load of neoplastic antebrachia was similar to those in 2 prior studies of surgical limb sparing techniques. The yield load (3145 N) exhibited by our neoplastic antebrachia was similar to that documented for antebrachia reconstructed with an endoprosthesis (3260 N),[28] and was greater than those after cortical bone grafting (2225 N),[28] vascularized ulnar transposition grafting (1179 N),[34] and radial grafting simulating cortical grafting (1901 N).[34] The mean maximum load sustained by neoplastic antebrachia in our

TABLE 1 Structural mechanical properties of neoplastic and unaffected bones

Structural variables	Neoplastic (n = 12) LSmean ± StdErr Median (Min, Max)	COV (%)	Control (n = 9) LSmean ± StdErr Median (Min, Max)	COV (%)	*P* value
Trot load					
Displacement (mm)	0.98 ± 0.14	54	0.61 ± 0.17	29	.132
Stiffness (kN/mm)	0.58 ± 0.07	43	0.76 ± 0.09	24	.150
Energy (kN*mm)	0.17 ± 0.02	64	0.15 ± 0.03	37	.487
Yield					
Displacement (mm)	3.69 ± 0.24	32	5.16 ± 0.28	16	***.002***
Load (kN)	3.15 (0.92, 8.00)	64	3.42 (3.00, 4.32)	14	.570
Stiffness (kN/mm)	1.12 (0.24, 2.62)	63	961 (0.65, 1.42)	16	.522
Energy (kN*mm)	5.89 ± 1.38	90	11.89 ± 1.64	24	***.020***
Maximum					
Displacement (mm)	6.15 ± 0.60	35	6.67 ± 0.71	19	.619
Load (kN)	3.58 ± 0.50	54	4.68 ± 0.60	13	.216
Energy (kN*mm)	12.66 (2.98, 28.50)	68	15.48 (9.51, 23.16)	26	.477
Failure					
Displacement (mm)	7.63 ± 0.96	46	9.92 ± 1.14	20	.179
Load (kN)	3.30 ± 0.43	52	4.03 ± 0.52	12	.336
Energy (kN*mm)	18.00 ± 4.54	85	31.19 ± 5.41	31	.107

The table include results of ANOVA, with Least Square Means (LSmean), Standard Error (StdErr), and Coefficient of Variation (COV) and results of the nonparametric statistical test, with Median (Min, Max) and COV. Comparisons shown in ***bold-italics*** are different at $P \leq .05$.

study (3581 N) was also similar to that documented in antebrachia reconstructed with an endoprosthesis (3445 N),[28] and was greater than those after cortical bone grafting (2446 N),[28] vascularized ulnar transposition grafting (1379 N),[34] and radial grafting simulating cortical grafting (2303 N).[34] Our study design precludes direct correlation between our results and clinical impact in clinical patients. However, comparing loads measured at failure in our neoplastic antebrachia to

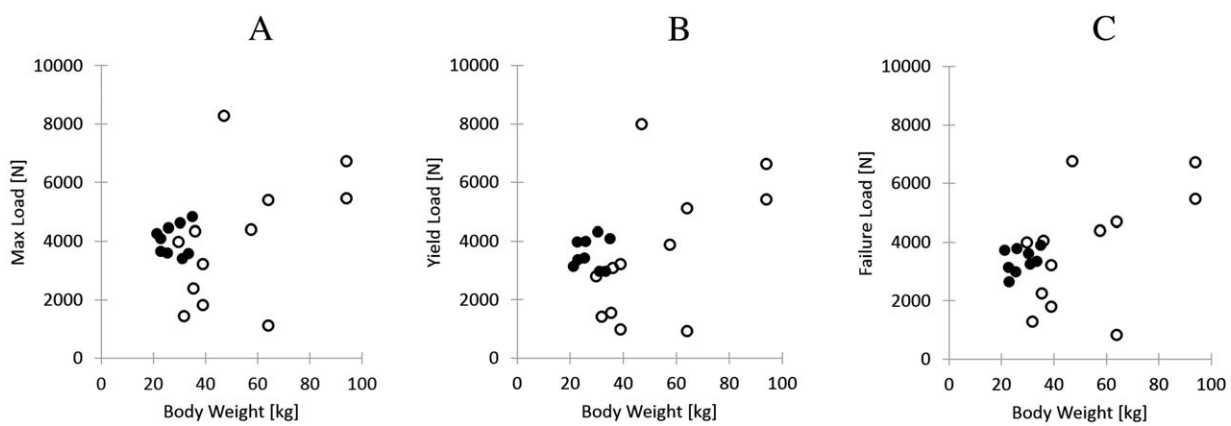

FIGURE 5 Scatter plots of yield load (A), maximum load (B), and failure loads (C) versus dog BW for neoplastic (filled circles) and control (open circles) antebrachii

TABLE 2 Normalized mechanical properties of neoplastic bones and unaffected bones

Normalized variables	Neoplastic (n = 12) LSmean ± StdErr Median (Min, Max)	COV (%)	Control (n = 9) LSmean ± StdErr Median (Min, Max)	COV (%)	*P* value
Trot load					
Displacement (mm/mm)	0.0049 (0.0027, 0.0138)	59	0.0035 (0.0023, 0.0042)	20	.059
Stiffness (N/mm/N/mm)	0.0071 ± 0.0012	60	0.0211 ± 0.0033	47	***.000***
Energy (N*mm/N*mm)	0.0019 (0.0012, 0.0057)	57	0.0020 (0.0011, 0.0027)	24	.972
Yield					
Displacement (mm/mm)	0.0215 ± 0.0012	20	0.0321 ± 0.0018	17	***<.001***
Load (N/N)	7.59 ± 1.26	58	14.57 ± 1.02	21	***.001***
Stiffness (N/mm/N/mm)	0.0124 ± 0.0027	76	0.0266 ± 0.0037	42	***.005***
Energy (N*mm/N*mm)	0.0764 ± 0.0149	67	0.2304 ± 0.0194	25	***<.001***
Maximum					
Displacement (mm/mm)	0.0336 ± 0.0037	38	0.0450 ± 0.0027	18	***<.001***
Load (N/N)	8.90 ± 1.37	53	16.50 ± 1.13	20	***.001***
Energy (N*mm/N*mm)	0.1557 ± 0.0250	56	0.4213 ± 0.0410	29	***<.001***
Failure					
Displacement (mm/mm)	0.0384 ± 0.0047	42	0.0654 ± 0.0050	23	***.001***
Load (N/N)	8.31 ± 1.20	50	13.67 ± 0.86	19	***.003***
Energy (N*mm/N*mm)	0.2093 ± 0.0414	68	0.7675 ± 0.0877	34	***<.001***

Load is normalized by BW, length by bone length, stiffness by BW/bone length, and energy by BW*bone length. The table includes results of ANOVA, with Least Square Means (LSmean), Standard Error (StdErr), and Coefficient of Variation (COV), and results of the nonparametric statistical test with Median (Min, Max) and COV. Comparisons shown in ***bold-italics*** are statistically different at $P \leq .05$.

those quoted above prompts us to suggest that the affected dogs in our study did not seem predisposed to pathological fractures compared to dogs undergoing limb salvage techniques.

The median yield load in our neoplastic antebrachia was higher than the peak vertical forces expected at a walk, trot, or jump. Based on force plate analysis, the peak vertical force of dogs has been estimated to 63% of body-weight while walking,[35] 110% of BW at the trot,[31-33] and 426% of BW while jumping over a 94 cm-high obstacle 94 cm high.[36] The mean normalized yield load (759% BW) in our neoplastic antebrachia was 12, 6.9, and 1.8 times higher than the peak vertical forces expected at a walk, trot, or jump. Comparing these values, we believe that neoplastic antebrachia in the current study would survive at least a single event of these activities.

Although neoplastic antebrachia allowed 28% less displacement and absorbed 50% less energy to yield than unaffected antebrachia, respectively, no difference was detected in pre-yield stiffness or any other associated biomechanical variables. These results may reflect the high variability of parameters measured in neoplastic antebrachii. This variability was likely related to differences in BW and bone size between dogs, as well as individual variability in the relative magnitude of destructive and proliferative activities within each tumor. When mechanical properties were normalized to BW and bone size, biomechanical properties of affected antebrachia were generally inferior to those of unaffected limbs; strength, stiffness, displacement, and energy were reduced in most affected specimen compared to controls. Increasing sample size in the diseased group may help better describe this cohort. In the meantime, our results support the concept that affected bones of dogs with OSA may have biomechanical properties allowing the rational consideration of in situ therapies.

Failure loads of bones with neoplastic bone loss depend on defect geometry, bone and neoplastic tissue material properties, and loading conditions. Consequently, estimates of reduction in bone strength or predictions of risk of failure are only moderately accurate, even for experienced physicians, with correlation coefficients between experimental measurements and expert predictions approximating 0.45-0.53.[37,38] Several in vitro studies have documented the determinant influence of bone architecture, measured by MR or CT imaging, on bone strength, independently of bone mineral density, and CT modeling has been found to improve predictions of pathologic fracture in humans.[39,40] Additionally, the risk of pathologic fracture depends on the mechanical properties of the whole bone but is also influenced by nonhomogeneous material density and structure in the OSA. These features create stress-risers during fatigue (high cycle) loading, raising the possibility that in vivo failure under further repetitive loading circumstances could occur at lower loads than the monotonic yield load observed in this study. Repeated loading gradually alters the mechanical properties of bone, promoting fatigue fractures when affected bone is unable to repair incurred damage.[41] The fatigue properties of neoplastic antebrachia were not evaluated in the current study.

Future research should therefore focus on cyclical loading models, as well as development of noninvasive methods to more empirically predict failure. Such studies would eventually allow stratification of dogs with distal radial bone tumors into higher and lower fracture risk groups. Patients at high risk for fracture may be better candidates for amputation or limb sparing procedures that reconstruct limb integrity with implants or grafts, whereas in situ therapies of diseased bone may be discouraged. However, a subset of patients may be identified as candidates for in situ treatments. This approach may also open up options for dogs with OSA affecting bones for which no surgical limb salvage options are currently established. Since distal radial bone tumors have recently been reported as less prone to pathologic fractures than bone tumors in other appendicular locations in dogs,[14] biomechanical testing of tumor-invaded bone in other anatomic locations is warranted to assess the viability of in situ techniques in other regions. Finally, difficulties controlling post-procedural weight bearing in quadrupeds such as dog also justify the development of preoperative assessment tools to determine the ability of the diseased bone to support the weight bearing forces. Such evaluation would guide the decision making of veterinarians considering in situ tumor treatment options for their patients. The results of this study lay the groundwork for further investigation in these areas.

ACKNOWLEDGMENTS

The authors are grateful to Mr Richard Larson for invaluable technical assistance in conducting this study. The described project was supported with funding from the University of California-Davis Center for Companion Animal Health.

CONFLICT OF INTEREST

The authors have no conflicts of interest to disclose.

REFERENCES

[1] Dernell WS, Ehrhart NP, Straw RC, Vail DM. Tumors of the skeletal system. In: Withrow SJ, Vail DM, eds. *Withrow and MacEwen's Small Animal Clinical Oncology*. 4th ed. St. Louis, MO: Elsevier; 2013:540-582.

[2] Liptak JM, Dernell W, Straw R, et al. Intercalary bone grafts for joint and limb preservation in 17 dogs with high-grade malignant tumors of the diaphysis. *Vet Surg.* 2004;33:457-467.

[3] Liptak JM, Dernell W, Ehrhart N, et al. Cortical allograft and endoprosthesis for limb-sparing surgery in dogs with distal radial osteosarcoma: a prospective clinical comparison of two different limb-sparing techniques. *Vet Surg.* 2006;35:518-533.

[4] Morello E, Vasconi E, Martano M, et al. Pasteurized tumoral autograft and adjuvant chemotherapy for the treatment of canine distal radial osteosarcoma: 13 cases. *Vet Surg.* 2003;32:539-544.

[5] Seguin B, Walsh PJ, Mason D, et al. Use of an ipsilateral vascularized ulnar transposition autograft for limb-sparing surgery of the distal radius in dogs: an anatomic and clinical study. *Vet Surg.* 2003;32:69-79.

[6] Ehrhart N. Longitudinal bone transport for treatment of primary bone tumors in dogs: technique description and outcome in 9 dogs. *Vet Surg.* 2005;34:24-34.

[7] Lascelles BDX, Dernell WS, Correa MT, et al. Improved survival associated with postoperative wound infection in dogs treated with limb-salvage surgery for osteosarcoma. *Annal Surg Oncol.* 2005;12:1073-1083.

[8] Mitchell KE, Boston SE, Kung M, et al. Outcomes of limb-sparing surgery using two generations of metal endoprosthesis in 45 dogs with distal radial osteosarcoma. A veterinary society of surgical oncology retrospective study. *Vet Surg.* 2016;45:36-43.

[9] Liptak JM, Dernell W, Lascelles BDX, et al. Intraoperative extracorporeal irradiation for limb sparing in 13 dogs. *Vet Surg.* 2004;33:446-456.

[10] Boston SE, Duerr F, Bacon N, et al. Intraoperative radiation for limb sparing of the distal aspect of the radius without transcarpal plating in five dogs. *Vet Surg.* 2007;36:314-323.

[11] Farese JP, Milner R, Thompson MS, et al. Stereotactic radiosurgery for treatment of osteosarcomas involving the distal portions of the limbs in dogs. *J Am Vet Med Assoc.* 2004;225:1567-1572.

[12] Walter CU, Dernell WS, LaRue SM, et al. Curative-intent radiation therapy as a treatment modality for appendicular and axial osteosarcoma: a preliminary

retrospective evaluation of 14 dogs with the disease. *Vet Comp Oncol.* 2005;3:1-7.

[13] Covey JL Farese JP, Bacon NJ, et al. Stereotactic radiosurgery and fracture fixation in 6 dogs with appendicular osteosarcoma. *Vet Surg.* 2014;43:174-181.

[14] Rubin JA, Suran JN, Brown DC, et al. Factors associated with pathological fractures in dogs with appendicular primary bone neoplasia: 84 cases (2007-2013). *J Am Vet Med Assoc.* 2015;247:917-923.

[15] Filippiadis DK, Tutton S, Kelekis A. Percutaneous bone lesion ablation. *Radiol Med.* 2014;119:462-469.

[16] Meller I, Weinbroum A, Bickels J, et al. Fifteen years of bone tumor cryosurgery: a single-center experience of 440 procedures and long-term follow-up. *Eur J Surg Oncol.* 2008;34:921-927.

[17] Mavrogenis AF, Rossi G, Rimondi E, et al. Palliative embolization for osteosarcoma. *Eur J Orthop Surg Traumatol.* 2014;24:1351-1356.

[18] Sabel MS. Cryo-immunology: a review of the literature and proposed mechanisms for stimulatory versus suppressive immune responses. *Cryobiology.* 2009;58:1-11.

[19] Joosten JJ, Muijen GN, Wobbes T, et al. In vivo destruction of tumor tissue by cryoablation can induce inhibition of secondary tumor growth: an experimental study. *Cryobiology.* 2001;42:49-58.

[20] Prehn RT. The inhibition of tumor growth by tumor mass. *Cancer Res.* 1991;51:2-4.

[21] Kaya M, Wada T, Nagoya S, et al. Concomitant tumour resistance in patients with osteosarcoma: a clue to a new therapeutic strategy. *J Bone Joint Surg Br.* 2004;86:143-147.

[22] Nishida H, Tsuchiya H, Tomita K. Reimplantation of tumour tissue treated by cryotreatment with liquid nitrogen induces anti-tumour activity against murine osteosarcoma. *J Bone Joint Surg Br.* 2008;90:1249-1255.

[23] Tsuchiya H, Wan S, Sakayama K, et al. Reconstruction using an autograft containing tumour treated by liquid nitrogen. *J Bone Joint Surg Am.* 2005;87:218-225.

[24] Boston SE, Bacon NJ, Culp WT, et al. Outcome after repair of a sarcoma-related pathologic fracture in dogs: a veterinary society of surgical oncology retrospective study. *Vet Surg.* 2011;40:431-437.

[25] Boston SE, Barry M, O'Sullivan ML. Transtumoral plating as a novel method for palliative limb spare and thromboembolism in a dog with a distal radial primary bone tumor. *Can Vet J.* 2011;52:650-655.

[26] Bhandal J, Boston SE. Pathologic fracture in dogs with suspected or confirmed osteosarcoma. *Vet Surg.* 2011;40: 423-430.

[27] Roe SC, Pijanowski GJ, Johnson AL. Biomechanical properties of canine cortical bone allografts: effects of preparation and storage. *Am J Vet Res.* 1988;49:873-877.

[28] Liptak JM, Ehrhart N, Santoni BG, et al. Cortical bone graft and endoprosthesis in the distal radius of dogs: a biomechanical comparison of two different limb spare techniques. *Vet Surg.* 2006;35:150-160.

[29] Coleman JC, Hart RT, Owan I, et al. Characterization of dynamic three-dimensional strain fields in the canine radius. *J Biomech.* 2002;35:1677-1683.

[30] Carter DR, Smith DJ, Spengler DM, et al. Measurement and analysis of in vivo bone strains on the canine radius and ulna. *J Biomech.* 1980;13:27-38.

[31] Garcia TC, Sturges BK, Stover SM, et al. Forelimb brachial muscle activation patterns using surface electromyography and their relationship to kinematics in normal dogs walking and trotting. *Compar Exercise Physiol.* 2014;10:13-22.

[32] Rumph PF, Lander J, Kincaid SA, et al. Ground reaction force profiles from force platform gait analyses of clinically normal mesomorphic dogs at the trot. *Am J Vet Res.* 1994;55:756-761.

[33] Kapatkin AS, Arbittier G, Kass PH, et al. Kinetic gait analysis of healthy dogs on two different surfaces. *Vet Surg.* 2007;36:605-608.

[34] Pooya HA, Seguin B, Mason DR, et al. Biomechanical comparison of cortical radial graft versus ulnar transposition graft limb-sparing techniques for the distal radial site in dogs. *Vet Surg.* 2004;33:301-308.

[35] Nielsen C, Stover SM, Schulz KS, et al. Two-dimensional link-segment model of the forelimb of dogs at a walk. *Am J Vet Res.* 2003;64:609-617.

[36] Yanoff SR, Hulse DA, Hogan HA, et al. Measurements of vertical ground reaction force in jumping dogs. *Vet Comp Orthop Traumatol.* 1992;5:44-50.

[37] Hipp JA, Springfiedl DS, Hayes WC. Predicting pathologic fracture risk in the management of metastatic bone defects. *Clin Orthop Relat Res.* 1995;312:120-135.

[38] Derikx L.C, van Aken J.B, Janssen D, et al. The assessment of the risk of fracture in femora with metastatic lesions: comparing case-specific finite element analyses with predictions by clinical experts. *J Bone Jt. Surg Br.* 2012;94:1135-1142.

[39] Bauer JS, Link TM. Advances in osteoporosis imaging. *Eur J Radiol.* 2009;71:440-449.

[40] Tanck E, van Aken JB, van der Linden YM, et al. Pathological fracture prediction in patients with metastatic lesions can be improved with computed tomography based computer models. *Bone.* 2009;45:777-783.

[41] Beaupied H, Lespessailles E, Benhamou CL. Evaluation of macrostructural bone biomechanics. *Joint Bone Spine.* 2007;74:233-239.

How to cite this article: Steffey MA, Garcia TC, Daniel L, Zwingenberger AL, and Stover SM. Mechanical properties of canine osteosarcoma-affected antebrachia. *Veterinary Surgery.* 2017;00:000-000. doi:10.1111/vsu.12628.